Choi and Auh *Applied Biological Chemistry* (2025) 68:39
https://doi.org/10.1186/s13765-025-01017-6

KSABC
The Korean Society for Applied Biological Chemistry

ARTICLE Open Access

Anti-diabetic potential of anthocyanin-rich fractions from purple-wheat (*Triticum aestivum* L.) cultivars and their correlation with metabolite profiles

Ye Jin Choi[1] and Joong-Hyuck Auh[1*]

Abstract
Wheat (*Triticum aestivum* L.) is a primary source of nutrition worldwide, and the development of wheat varieties with enhanced functionality has gained considerable interest. This study investigated the antidiabetic activities of three purple wheat varieties and their correlations with their metabolite profiles. We evaluated the antioxidant and antidiabetic activities of the anthocyanin-rich fractions derived from these cultivars. Anthocyanins were extracted from wheat bran using acidified 80% methanol and purified using ion-exchange chromatography. The metabolites were analyzed using UHPLC-HESI-Orbitrap MS/MS. Antioxidant capacity was evaluated by measuring the total polyphenol content and analyzing DPPH, ABTS, ORAC, and ROS levels. Antidiabetic activity was determined through α-glucosidase inhibition and glucose uptake in insulin-resistant HepG2 cells. The effect on the PI3K/AKT signaling pathway was investigated using western blot analysis. The "Ari-heukchal" cultivar exhibited the highest total polyphenol content, antioxidant capacity, and α-glucosidase inhibitory activity. Treatment of insulin-resistant HepG2 cells with 200 μg/mL of the anthocyanin-rich fraction improved glucose uptake and significantly increased AKT phosphorylation at Ser473. This effect was attributed to the high anthocyanin content in the "Ari-heukchal" cultivar. The findings support the potential use of natural anthocyanin pigments from purple-wheat cultivars for the development of functional materials from colored grains.

Keywords Colored wheat, Ariheuk, Anthocyanin-rich fraction, Antioxidant, Anti-diabetic

Introduction

Wheat (*Triticum aestivum*) is a major grain crop belonging to the Poaceae (Gramineae) family and serves as a primary global food source. Approximately 772 million tons of wheat-based food products, including pasta, crackers, noodles, and pastries, are produced annually in more than 120 countries [1]. However, in Korea, the domestic wheat self-sufficiency rate is only 1%, relying heavily on imports. To address this challenge, the Korean government is providing farmers with customized, functional wheat cultivars to enhance both the value and productivity of wheat cultivation [2].

The Rural Development Administration of Korea developed the purple-wheat cultivar "Ariheuk" by crossing "Heuk2 (K253305)" with "Sinmichal (IT215851)" [3]. "Ariheuk" is characterized by its dark red color and contains higher levels of anthocyanin, tannin, and polyphenols than regular wheat, resulting in antioxidant capacity

*Correspondence:
Joong-Hyuck Auh
jhauh@cau.ac.kr
[1]Department of Food Science and Biotechnology, Chung-Ang University, Anseong 17546, Republic of Korea

approximately 10 times greater than that of conventional wheat [2]. Additionally, the cultivars "Ari-jinheuk" and "Ari-heukchal" were developed by crossing "Heukmil" with "Heukripsomaek76 (IT229974)" and the resulting cultivar with "Sinmichal". The amylose and amylopectin content varies across these cultivars.

Colored wheat, including purple, blue, and black wheat cultivars, depending on the location of the anthocyanins, originates from conventional species or breeding processes [4]. Purple-wheat, such as "Ariheuk", contains anthocyanin in the pericarp layer. These water-soluble flavonoids, derived from anthocyanidins, exhibit anticancer, anti-inflammatory, antibacterial, and antidiabetic properties [5].

Anthocyanin-rich berries exhibit excellent antioxidant activity, with extracts that significantly inhibit various human tumor cells [6]. Mulberry-derived purified anthocyanins increase glucose consumption and improve insulin resistance (IR) in insulin-resistant HepG2 cells and db/db mice [7].

Unlike fruit-based anthocyanin sources, purple wheat supplies these pigments within a matrix rich in starch and dietary fiber, which can be consumed daily through staple foods such as bread, noodles, and breakfast cereals. Clinical studies have shown that bread made from purple wheat lowers the glycemic index and attenuates post-prandial plasma glucose levels [8]. In the present study, an anthocyanin-rich fraction was isolated from purple wheat bran, a milling by-product that constitutes approximately 14% of the grain and is produced in quantities exceeding 150 million tons annually worldwide [9, 10]. These characteristics indicate that anthocyanins obtained from purple wheat bran represent an economical and practical functional ingredient for the long-term dietary control of glycemia.

Type 2 diabetes mellitus (T2DM) is a metabolic disease characterized by hyperglycemia, IR, and relative insulin deficiency, which impair glucose transport to the liver, muscle cells, and fat cells [11]. The liver plays a central role in glucose metabolism and is regulated by insulin through a complex signaling pathway [12]. The insulin receptor substrate proteins, IRS-1 and IRS-2, activate phosphatidylinositol 3-kinase (PI3K), which subsequently activates AKT through phosphorylation, which is a crucial step in the regulation of glucose metabolism [7, 13].

The International Diabetes Federation has projected that the diabetic population will reach 783 million by 2045. Current T2DM treatments involve chemical agents, such as biguanides, sulfonylureas, and thiazolidinediones; however, these drugs are associated with side effects, such as obesity and edema [14]. Consequently, there is a growing interest in natural products with antidiabetic activity [15].

However, there is limited research on the antidiabetic activity of anthocyanins isolated from colored Korean wheat. Therefore, in this study, we aimed to determine the effects of wheat-derived anthocyanin-rich fractions on AKT signaling pathway-mediated blood glucose regulation in HepG2 cells. Additionally, we aimed to determine the antioxidant activity of the wheat-derived anthocyanin-rich fractions and identify the metabolites underlying the role of wheat-induced blood glucose regulation.

Results

Preparation of anthocyanin-rich fractions from purple-wheat cultivars

Purple-wheat cultivars ("Ariheuk", "Ari-jinheuk", and "Ari-heukchal") were milled, and the bran fraction was isolated for extraction. The defatted bran was extracted using 80% acidified methanol with 0.1% hydrochloric acid via sonication. The extraction was followed by centrifugation, filtration, and concentration. The anthocyanin-rich fraction was purified using Amberlite XAD-7HP resin and eluted with acidified methanol. On a dry weight basis, the crude extract yield was the highest in AHC (8.91 ± 0.22%), followed by AJH (8.33 ± 0.31%) and AH (7.02 ± 0.20%). Similarly, the anthocyanin-rich fraction yield varied slightly, ranging from 2.08 ± 0.18% in AH to 2.36 ± 0.30% in AHC, with AJH exhibiting 2.35 ± 0.04%.

Measurement of phytochemical content

The total phenolic compounds (TPC) content in the anthocyanin-rich fractions from the three purple wheat cultivars were determined using the Folin and Ciocalteu's phenol reagent method, as shown in Table 1. The highest phenolic content was observed in AHC with 40.43 mg GAE/g, followed by AH and AJH.

The total flavonoid content (TFC) of the anthocyanin-rich fractions from the three purple-wheat

Table 1 Total phytochemical content of anthocyanin-rich fractions from three purple-wheat cultivars

Sample	Total phenolic content (mg of GAE/g of sample)	Total flavonoid content (mg of QE/g of sample)	Total anthocyanin content (mg C3OG/g)
AH	37.49 ± 0.33^{b}	16.94 ± 0.53^{c}	1.04 ± 0.03^{b}
AJH	32.57 ± 0.32^{c}	19.21 ± 0.27^{b}	0.81 ± 0.01^{c}
AHC	40.43 ± 0.39^{a}	20.32 ± 0.23^{a}	1.15 ± 0.02^{a}

Each value represents the mean ± SD from three separate experiments. Different letters indicate significant differences ($p < 0.05$)

AH, Ariheuk; AJH, Arijinheuk; AHC, Ariheukchal

cultivars is summarized in Table 1. The TFC value for AHC (20.32 mg QE/g) was significantly higher than that of TPC. However, the TFC in AJH was higher than that in AH.

Total anthocyanin content (TAC) of anthocyanin-rich fractions from the three purple wheat cultivars, determined using the pH-differential method are shown in Table 1. The TAC was the highest in AHC (1.15 mg C3OG/g), followed by AH (1.04 mg C3OG/g) and AJH (0.81 mg C3OG/g). Notably, the anthocyanin-rich fraction obtained in this study had an anthocyanin content approximately eight times higher than the reported total anthocyanin content of the "Ariheuk" cultivar (0.127 mg/g), as reported by the Rural Development Administration (RDA) [16].

Metabolomic characterization of anthocyanin-rich fractions from purple-wheat cultivars

Metabolomic profiling of the three purple-wheat cultivars was conducted using UHPLC-HESI orbitrap-MS/MS data. The analysis was performed in the positive ion mode, and multivariate statistical analyses were applied to distinguish metabolite patterns across cultivars. Heatmap analysis of the 266 metabolomes revealed variations in the relative concentrations of key metabolites among the three purple wheat cultivars (Fig. 1A). Further multivariate analyses, including principal component analysis (PCA), were used to identify differences in metabolites among the purple-wheat cultivars. The PCA results, illustrated by principal components 1 (PC1) and 2 (PC2), explained 76.6% and 21.9% of the variance, respectively, and displayed distinct clusters. Specifically, AHC was differentiated from the other two cultivars based on PC1, whereas AH and AJH were separated by PC2 (Fig. 1B). Hierarchical clustering analysis (HCA) was used to

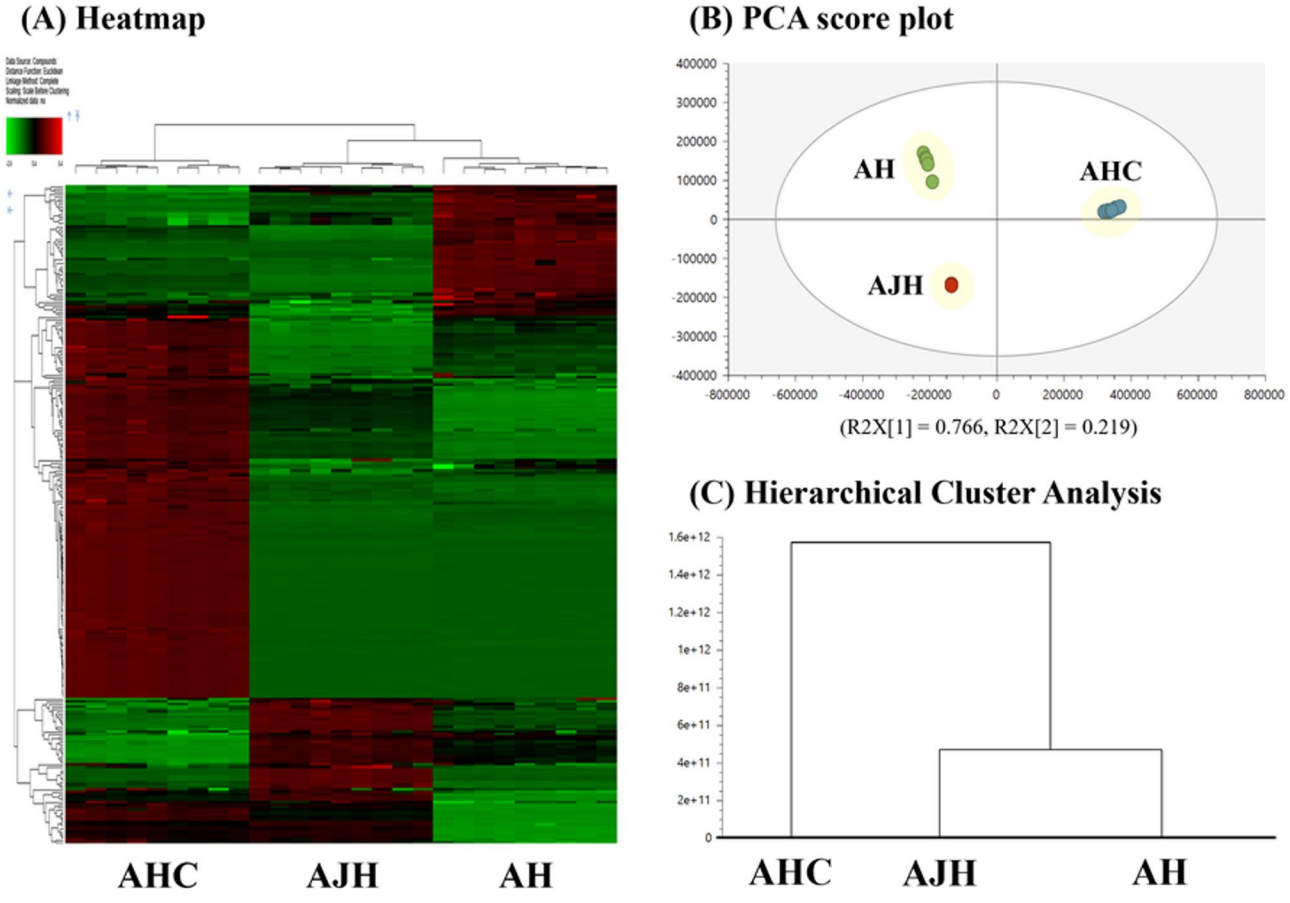

Fig. 1 Heatmap analysis, PCA score plot and HCA of metabolites in anthocyanin-rich fractions from three purple-wheat cultivars. (**A**) The cultivars are represented by columns, and the values of the 266 detected metabolites are represented by rows. The analysis was conducted in positive ion mode using an Orbitrap mass analyzer. The light green and red colors indicate relatively low and high content, respectively. Nine replicates were used for metabolite analysis. (**B**) The hierarchal clustering analysis (HCA) shows that based on PC1, AHC is distinct from the other two cultivars, which accounts for 76.6% of the variance. Meanwhile, AH and AJH are separated based on PC2, which explains 21.9% of the variance. (C) The consistency in metabolite patterns within each group further confirms the distinctions observed in the PCA score plot. AH, Ariheuk; AJH, Ari-jinheuk; AHC, Ari-heukchal

Table 2 Content of signature metabolites in anthocyanin-rich fractions from three purple-wheat cultivars

Sample	Cyanidin-3-O-glucoside (μg/g)	Peonidin-3-O-glucoside (μg/g)	Cyanidin (μg/g)	Cyanidin-3-rutinoside (μg/g)
AH	231.73 ± 7.53[b]	103.82 ± 2.77[c]	36.22 ± 0.57[b]	52.93 ± 0.63[a]
AJH	227.64 ± 1.63[b]	173.28 ± 1.09[b]	60.12 ± 0.55[a]	48.93 ± 0.20[b]
AHC	345.07 ± 4.10[a]	316.43 ± 3.41[a]	36.85 ± 0.03[b]	48.68 ± 0.14[b]

Each value represents the mean ± SD from three separate experiments. Different letters indicate significant differences ($p < 0.05$)

AH, Ariheuk; AJH, Arijinheuk; AHC, Ariheukchal

Table 3 Antioxidant activity of anthocyanin-rich fractions from three purple-wheat cultivars

Sample	DPPH IC 50 (mg/mL)	ABTS (μM TE/mg)	ORAC (μM TE/mg)
AH	0.266 ± 0.01[b]	212.24 ± 0.46[c]	1515.39 ± 33.89[b]
AJH	0.246 ± 0.005[a]	219.55 ± 0.33[b]	1440.29 ± 9.74[b]
AHC	0.235 ± 0.007[a]	262.13 ± 3.10[a]	2176.24 ± 52.28[a]

Each value represents the mean ± SD from three separate experiments. Different letters indicate significant differences ($p < 0.05$)

AH, Ariheuk; AJH, Arijinheuk; AHC, Ariheukchal

categorize cultivars based on similar metabolite profiles (Fig. 1C), further confirming the distinct metabolomic patterns.

Quantification of anthocyanins in purple-wheat cultivars

The main anthocyanins found in "Ariheuk" are cyanidin-3-O-glucoside (C3G) and peonidin-3-O-glucoside (P3G) [16]. Additionally, previous studies have confirmed that cyanidin and peonidin are significantly more abundant among the six anthocyanin types, with cyanidin-3-glucoside being the dominant pigment (45.8%), followed by peonidin-3-glucoside (20.2%) and cyanidin-3-rutinoside (6.5%) [17]. Therefore, in this study, anthocyanin content was quantified using the parallel reaction monitoring (PRM) mode. In this study, three anthocyanins (cyanidin-3-O-glucoside, peonidin-3-O-glucoside, and cyanidin-3-O-rutinoside) were quantified, along with cyanidin (anthocyanidin). Non-targeted metabolite analysis detected cyanidin-3-glucoside, peonidin-3-glucoside, cyanidin-3-rutinoside, and cyanidin (data not shown).

Cyanidin-3-O-glucoside was the primary anthocyanin detected across all three purple-wheat cultivars, with a significantly high AHC concentration (345.07 ± 4.10 μg/g) (Table 2). Peonidin-3-O-glucoside also had a significantly higher AHC content (316.43 ± 3.41 μg/g) than the other two cultivars.

Additionally, an OPLS-DA model was constructed using only the four targeted anthocyanins to assess their discriminative power among the cultivars. Variable Importance in Projection (VIP) values were calculated to evaluate the relative contribution of each compound. Peonidin-3-O-glucoside (P3OG) showed the highest VIP value (1.664), possibly reflecting its high abundance and strong bioactivity, as further supported by the antioxidant and antidiabetic assay results described below. The VIP values of other anthocyanins, such as cyanidin-3-O-glucoside (0.979), cyanidin (0.492), and cyanidin-3-O-rutinoside (0.172), were lower than that of P3OG.

Antioxidant activity of anthocyanin-rich fractions

The DPPH free radical-scavenging activities of the anthocyanin-rich fractions are shown in Table 3. For each fraction, the results were expressed as IC50 values, indicating the concentration required to remove 50% of the DPPH radicals. The IC50 values of AJH and AHC were significantly lower than that of the cultivar AH, suggesting that the anthocyanin-rich fractions of AJH and AHC exhibited a higher DPPH radical scavenging effect. (data not shown for standard ascorbic acid: 0.005–0.0002 mg/ml).

The ABTS radical-scavenging activities of the anthocyanin-rich fractions are shown in Table 3. AHC (262.13 ± 3.10 μM TE/mg) exhibited the highest ABTS radical scavenging potential among the three cultivars, significantly outperforming AJH and AH.

Oxygen radical absorbance (ORAC) values of the anthocyanin-rich fractions are listed in Table 3. Similar to the DPPH and ABTS results, the ORAC value was also significantly higher in AHC (2176.24 ± 52.28 μM TE/mg) than that in the other two cultivars.

Cytotoxicity of anthocyanin-rich fraction in HepG2 cells

The effect of the anthocyanin-rich fraction on HepG2 cell viability was evaluated using an MTT assay. Fractions from three cultivars, AH, AJH, and AHC, were tested at concentrations of 100, 200, and 400 μg/mL. HepG2 cell proliferation was considered affected if cell viability dropped below 80%. The cells treated with purified anthocyanin-rich fraction maintained cell viability above 80% (ranging from 96.63 ± 1.36% to 122.82 ± 2.51%) at all tested concentrations for the three cultivars. The three cultivars tended to increase cell viability in a concentration-dependent manner, which contributed to the

establishment of suitable concentrations for subsequent experiments.

Effect of anthocyanin-rich fraction on intracellular reactive oxygen species (ROS) levels

In this study, IR was induced by treating cells with 1 μM insulin in a 25 mM glucose medium. The intracellular ROS production level of the anthocyanin-rich fraction was assessed and is shown in Fig. 2.

The anthocyanin fractions from three purple-wheat cultivars were tested at concentrations of 100, 200, and 400 μg/mL. AJH and AHC lead to a 50% reduction in intracellular ROS production compared to the control group (INS). Similarly, AH lead to a 15% reduction in intracellular ROS production. Although ROS did not decrease in a concentration-dependent manner, we found that the lowest ROS levels in all three cultivars occurred at 200 μg/mL. Therefore, further experiments were performed at 200 μg/mL.

Antidiabetic activity of anthocyanin-rich fraction

The α-glucosidase inhibitory activity of anthocyanin-rich fractions from the three purple-wheat cultivars was assessed at 200 μg/mL using a colorimetric method. AHC (1.01 ± 0.03 mg/mL) exhibited a significantly lower IC50 value than AH (1.17 ± 0.12 mg/mL) and AJH (1.15 ± 0.06 mg/mL), indicating the strongest inhibitory effect on α-glucosidase activity. Acarbose, a well-known α-glucosidase inhibitor, served as the positive control and had an IC50 of 0.27 ± 0.06 mg/mL (data not shown).

To evaluate the IR in HepG2 cells, a glucose uptake assay was conducted. A model of IR was established by mimicking hyperglycemia and hyperinsulinemia in HepG2 cell cultures. Glucose uptake analysis revealed that the absorption rate in the group treated with a high insulin concentration in a high-glucose medium was significantly reduced compared to that in the group treated with low-glucose medium (Fig. 3A). These results demonstrated that IR was successfully induced in HepG2 cells under high glucose and high insulin treatment conditions.

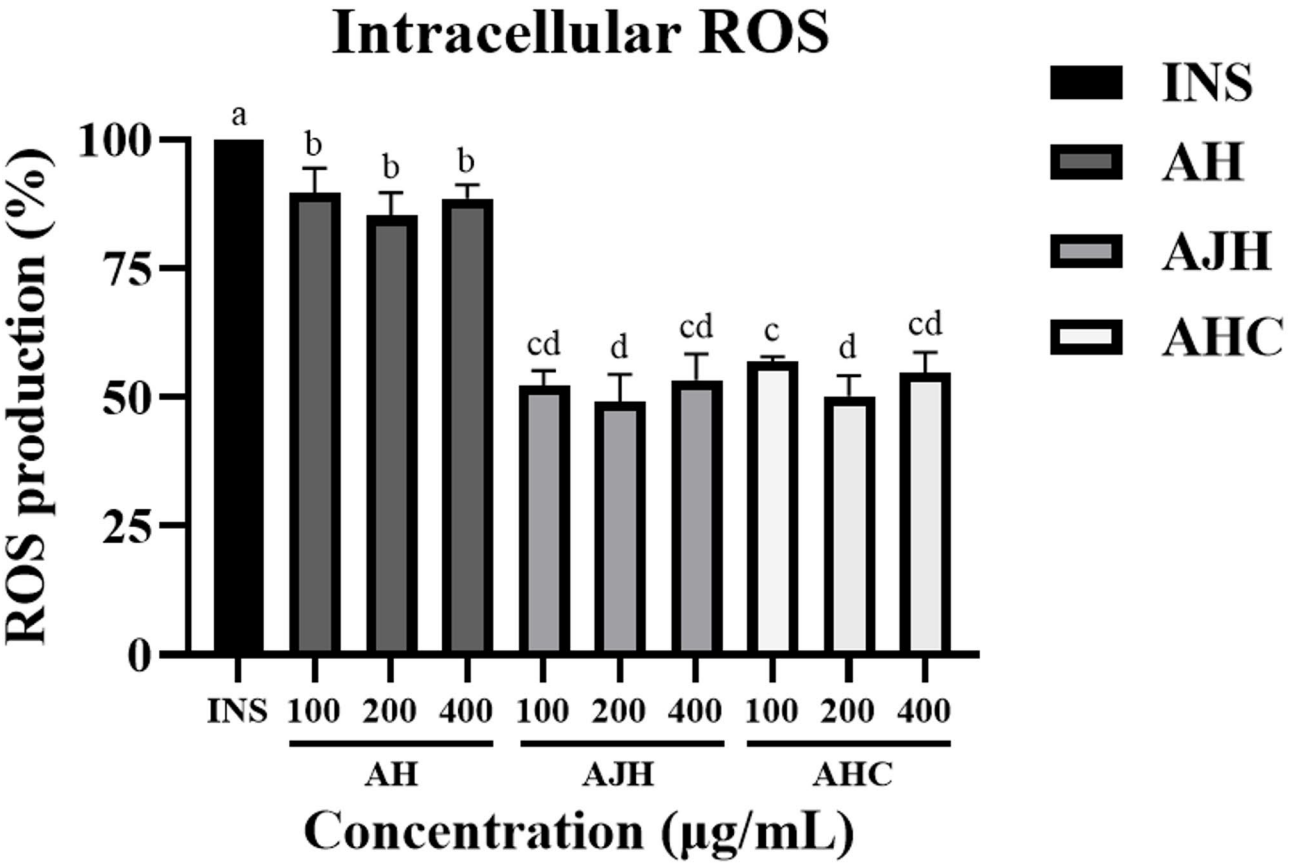

Fig. 2 Intracellular ROS scavenging activity of anthocyanin-rich fractions from three purple-wheat cultivars. Insulin-resistant Hepg2 cells were treated with 100, 200, and 400 μg/mL for 24 h and then stimulated with insulin (100 nM) for 20 min. Subsequently, the cells were incubated with CM-H2DCFDA (10 μM) for 30 min and washed thoroughly with DPBS. Different letters indicate significant differences ($p < 0.05$). Intracellular ROS levels were expressed as a percentage of control cells (INS). AH, Ariheuk; AJH, Ari-jinheuk; AHC, Ari-heukchal

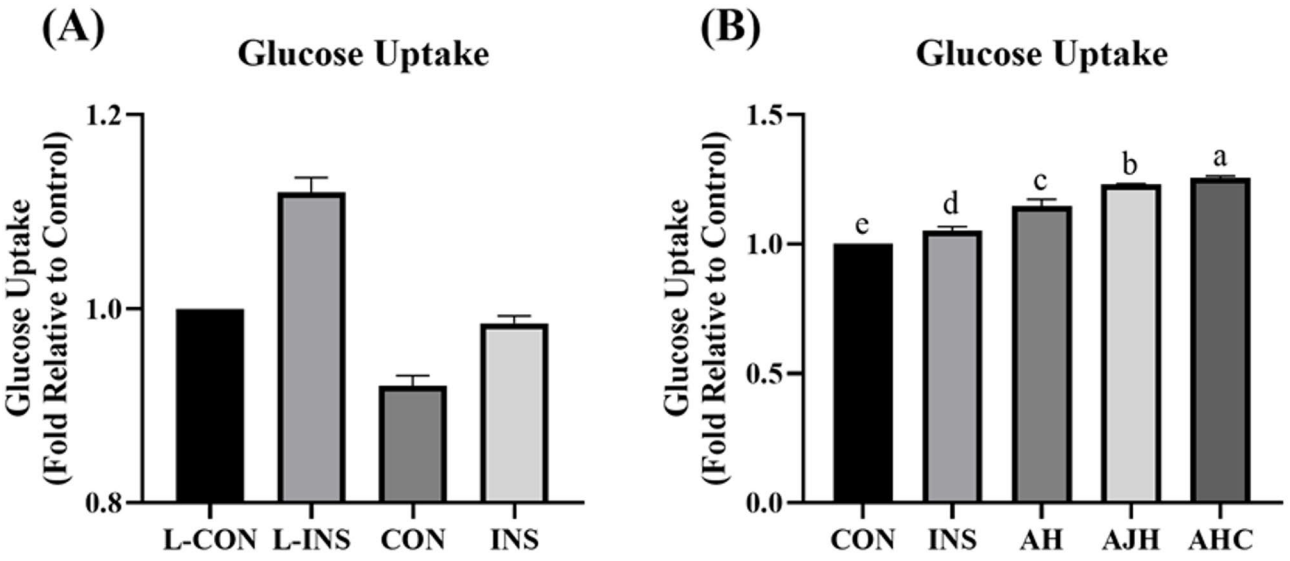

Fig. 3 Effect of anthocyanin-rich fractions from three purple-wheat cultivars on glucose uptake in HepG2 cells. (**A**) Glucose uptake in HepG2 cells was compared by incubating cells in medium with different glucose concentrations (5.5 or 25 mM) and insulin treatment (presence or absence). L-CON, 5.5 mM glucose DMEM; L-INS, 5.5 mM glucose DMEM + Insulin 100 nm treatment; CON, 25 mM glucose DMEM; INS, 25 mM glucose DMEM + Insulin 100 nm treatment. (**B**) Quantitative analysis of glucose uptake was performed by measuring bioluminescence. Cells were treated with 1 mM 2-deoxyglucose (2DG), and the uptake was terminated. A detection reagent was added and incubated for 1 h, followed by luminescence measurement using a luminometer. Each value represents the mean ± SD from three independent experiments. AH, Ariheuk; AJH, Ari-jinheuk; AHC, Ari-heukchal

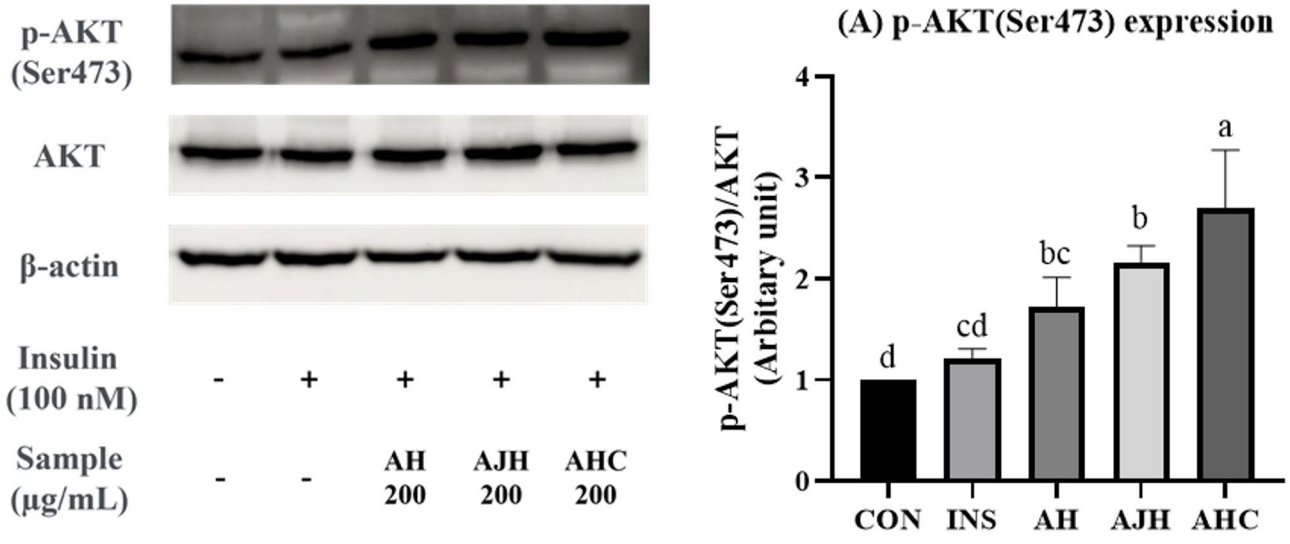

Fig. 4 Effect of anthocyanin-rich fractions from three purple-wheat cultivars on AKT phosphorylation in HepG2 cells. Insulin-resistant Hepg2 cells were treated with 200 μg/mL of anthocyanin-rich fractions for 24 h and then stimulated with insulin (100 nM) for 20 min. (**A**) p-AKT (Ser 473) expression was quantified. AH, Ariheuk; AJH, Ari-jinheuk; AHC, Ari-heukchal

The effect of the anthocyanin-rich fraction on glucose uptake by insulin-resistant HepG2 cells was assessed using a 2DG-based bioluminescent glucose uptake assay. Subsequently, each of the three types of anthocyanin-rich fractions was treated at a concentration of 200 μg/mL to measure and compare luminescence. Among the samples, AHC (1.26 ± 0.011) treatment resulted in the most significant increase in glucose uptake compared to the control group (Fig. 3B). Similarly, treatments with AJH (1.23 ± 0.002) and AH (1.15 ± 0.022) also enhanced glucose uptake.

The level of phospho-Akt (Ser473) was assessed and compared with total Akt protein levels. The results, illustrated in Fig. 4, suggest that the anthocyanin-rich fractions from the three purple-wheat cultivars activated the AKT pathway. When compared to insulin treatment alone, the addition of anthocyanin-rich fractions significantly increased the phosphorylation of Ser473

(Ins: 1.21 ± 0.07, AH: 1.72 ± 0.24, AJH: 2.16 ± 0.14, AHC: 2.7 ± 0.47). Additionally, among the three cultivars, the expression of phospho-Akt (Ser473) was most significantly enhanced in the AHC-treated group. This suggests that the anthocyanin-rich fractions, particularly AHC, effectively activate the PI3K/AKT signaling pathway, improve liver IR, and regulate glucose metabolism.

Correlation between anthocyanin content and bioactivity

As shown in the heat map (Fig. 5), peonidin-3-O-glucoside (P3OG) exhibited strong positive correlations with multiple endpoints including total flavonoid content (TFC), ABTS and ORAC antioxidant capacity, p-AKT(Ser473) expression, and glucose uptake. Similarly, cyanidin-3-O-glucoside (C3OG) showed notable associations with α-glucosidase inhibition and other antioxidant measures. It is important to note that DPPH, ROS, and α-glucosidase results were expressed as IC_{50} values, where lower IC_{50} indicates higher bioactivity. Consequently, the negative correlations observed in these assays should be interpreted as strong inverse relationships, suggesting that higher anthocyanin concentrations lead to greater functional activity. Taken together, these Spearman correlation results highlight P3OG and C3OG as the most functionally relevant anthocyanins, consistent with their relative abundance in the AHC and AH cultivars, respectively. This provides further evidence supporting the contribution of specific anthocyanin profiles to the bioactivity of purple wheat fractions.

Discussion

In this study, anthocyanins were purified from wheat bran of the functional purple-wheat cultivars: Ariheuk, Ari-jinheuk, and Ari-heukchal, to prepare anthocyanin-rich fractions. The crude extract was prepared using acidified methanol and then purified using column chromatography. Acidified methanol was selected as the most effective solvent for anthocyanin extraction [18]. Previous studies have shown that column chromatography is an efficient method for isolating and purifying high-purity anthocyanins from crude extracts [19].

The antioxidant and antidiabetic activities of these fractions were measured, and significant metabolites among the cultivars were identified using LC-MS/MS analysis. Untargeted metabolomics analysis was initially performed because no prior studies have reported metabolomic differences among Korean purple wheat cultivars. Furthermore, the experimental samples used in this study were all derived from purple wheat and differed only in cultivar. To explore cultivar-specific metabolic variations, PCA and HCA were first employed as part of the untargeted approach. Subsequently, targeted analysis was conducted for four major anthocyanins known to be key bioactive compounds in purple wheat. The multivariate statistical analysis revealed clear differences in metabolite profiles among the cultivars. Although S-plots were used during preliminary data exploration to further distinguish group separation, the four targeted anthocyanins were consistently present in all three cultivars and therefore were not identified as top discriminative variables in the untargeted dataset. Accordingly, the study focused on visualizing and interpreting overall metabolic patterns through untargeted analysis and assessing the

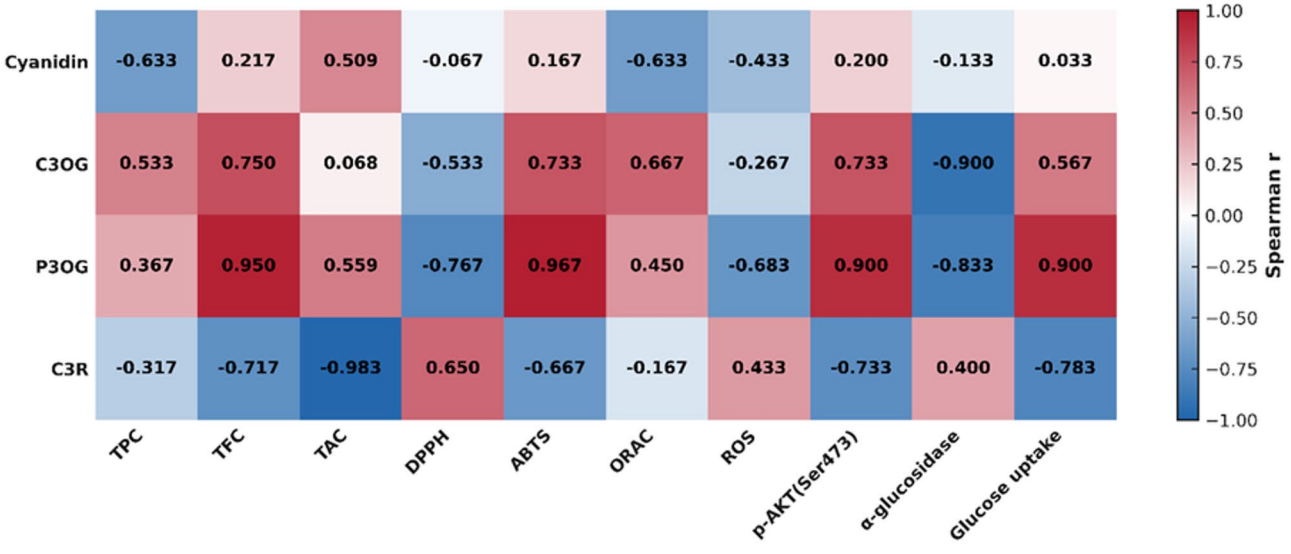

Fig. 5 Spearman's correlation between major anthocyanin contents and bioactivity assay results. Peonidin-3-O-glucoside (P3OG) exhibited strong positive correlations with multiple endpoints. The results for DPPH, ROS, and α-glucosidase were expressed as IC_{50} values; therefore, although the correlation coefficients may appear negative, these reflect inverse. C3OG, Cyanidin-3-O-glucoside; P3OG, Peonidin-3-O-glucoside; C3R, Cyanidin-3-O-rutinoside

Table 4 Tentative identification of the key anthocyanin compounds from purple-wheat cultivars

m/z	RT (min)	Tentative identification	MS/MS fragments	Mass error (ppm)
287.0538	10.91	Cyanidin	287.05 288.05 137.02	-4.18
449.1065	8.07	Cyanidin-3-O-glucoside	287.05 288.05 137.02	-2.97
463.1219	9.18	Peonidin-3-O-glucoside	301.07 302.07 286.04	-3.42
595.1616	8.55	Cyanidin-3-rutinoside	287.05 288.08 289.05	2.68

functional relevance of the four anthocyanins through targeted quantification. Finally, correlation analysis was performed between the quantified levels of these anthocyanins and the results of antioxidant and antidiabetic assays, providing additional evidence that specific anthocyanin profiles contribute to the bioactivity of purple wheat fractions.

Major anthocyanin compounds were quantified using the PRM mode, which isolates and fragments the target precursor ion while monitoring all the MS/MS fragment ions generated in parallel. This method provides excellent selectivity and sensitivity, enabling the detection of highly reliable quantitative results [20, 21].

Identification of the four target anthocyanins was based on their precursor ion m/z values, retention times, and characteristic MS/MS fragmentation patterns, which were compared against reference spectra from public databases including mzCloud, MoNA, PubChem, and MASSBANK (Table 4).

When comparing the major anthocyanin content, the fractions purified from normal wheat bran had barely detectable levels of cyanidin-3-O-glucoside and peonidin-3-O-glucoside. Their concentrations were approximately 29–39 times lower than those found in the AHC cultivar, which showed the highest levels among the purple wheat cultivars (data not shown). Therefore, this confirmed the successful purification of the anthocyanins.

When comparing the anthocyanin content of purple-wheat with the quantitative amounts reported in previous studies [17, 22], notable differences were observed. These discrepancies are likely due to the influence of extraction and purification conditions on anthocyanin content and composition. Additionally, anthocyanin pigment content and composition can vary from year to year, even within the same cultivar, with significant effects arising from interactions among genotype, year, and location [23–25].

Among the three cultivars, AHC exhibited the highest TPC, TFC, and TAC content, and demonstrated significantly greater antioxidant capacity in both ABTS and ORAC assays. Previous studies have shown that cultivars with the highest total flavonoid and anthocyanin contents among various colored whole wheat cultivars tend exhibited high DPPH and ORAC values, indicating a correlation between flavonoids and antioxidant activity [26].

Additionally, AHC and AJH reduced intracellular oxidative stress levels by approximately 50%. Previous studies have shown that elevated ROS levels in HepG2, induced by high glucose and insulin conditions, contribute to the development of IR [27]. Therefore, reducing ROS production in HepG2 cells is essential for maintaining cellular function.

Oxidative stress plays a key role in various diseases, particularly in diabetes mellitus. It disrupts the cellular oxidative state and redox balance, leading to IR, beta-cell dysfunction, impaired glucose tolerance, and mitochondrial dysfunction [28].

In a previous study, anthocyanins purified from *Lycium ruthenicum* significantly reduced ROS levels in insulin-resistant HepG2 cells, exhibiting inhibitory effects similar to that of metformin [29]. Another study found that treatment of HepG2 cells with cyanidin-3-O-glucoside led to a dose-dependent reduction in ROS levels, with a 68% reduction at the highest dose (100 μM) [30]. These findings suggest that the anthocyanins in AJH and AHC, which significantly reduced ROS levels, effectively inhibited ROS production.

The α-glucosidase inhibitory activity of AHC was higher than that of the other two cultivars, indicating its strong antidiabetic potential. In a similar study, anthocyanins purified from purple corn cobs showed an IC 50 value of 1.221 ± 0.141 mg/mL for α-glucosidase inhibition [31], which is consistent with the antidiabetic activity observed in the present study.

In hepatocytes, IR is likely caused by a combination of pathological factors, such as hyperglycemia, hyperinsulinemia, advanced glycation end products, elevated free fatty acids and their metabolites, and oxidative stress [32]. These factors lead to reduced insulin sensitivity, resulting in decreased glucose uptake by peripheral tissues and diminished inhibition of hepatic glucose production.

These findings confirmed that IR was effectively induced in HepG2 cells under high glucose and high insulin treatment conditions.

Previous studies have shown that glucose uptake significantly increased in insulin-resistant HepG2 cells treated with 100 μg/mL of proanthocyanidins from Chinese bayberry leaves [33]. Similarly, treatment with 50, 100, and 150 μg/mL of mulberry anthocyanin extracts in insulin-resistant HepG2 cells induced by high glucose and palmitic acid resulted in increased glucose uptake [7]. These findings suggest that anthocyanin-rich fractions can effectively increase glucose uptake by insulin-resistant HepG2 cells.

The PI3K/AKT signaling pathway, a crucial insulin signaling pathway, promotes glucose utilization in various tissues, including the regulation of glucose metabolism in the liver, including processes, such as glycogen synthesis and gluconeogenesis [34].

Akt phosphorylation induces the expression and translocation of GLUT4 from the cytoplasm to the cell membrane, thereby enhancing glucose uptake [35]. The glucose uptake activity and Akt phosphorylation levels of the samples, as shown in Figs. 3B and 4, demonstrated a similar proportional increase to those observed in previous studies.

According to a previous study that evaluated glucose uptake using 2-NBDG in L6 skeletal muscle cells, treatment with 20 μM of C3OG increased the glucose uptake rate by 78.10%, with a 4.95 times increase in p-AKT (Ser473)expression, showing a 2.78-fold difference in the upregulation rate between the two measurements [35]. Additionally, treatment with black soybean seed extract at 150 μg/mL increased the glucose uptake rate by 81.24%, with p-AKT (Ser473) expression increased by 4.12 times, resulting in a 2.27-fold difference in the upregulation rate between the two measurements [35]. In this study, the glucose uptake rate in cells treated with AHC increased 1.26 times, while the expression of p-AKT (Ser473) increased by 2.70 times. This resulted in a 2.14-fold difference in the upregulation rate, which is consistent with the findings of previous studies.

In previous studies measuring glucose uptake in HepG2 cells, treatment with 400 μg/mL of purple corn pericarp extract obtained through column purification increased glucose uptake by 45% [36]. The same study found that treatment with 100 μM P3OG and C3OG increased HepG2 cellular glucose uptake by 19% and 31%, respectively. In this study, treatment with 200 μg/mL of AHC increased glucose uptake by 26%, showing a similar uptake increase to those observed in a previous study. Additionally, in a previous study that examined the expression of p-AKT (Ser473) in HepG2 cells cultured in high-glucose medium, AKT phosphorylation increased by 2.79 times when treated with 50 μM of C3OG [37]. In this study, treatment of insulin-resistant HepG2 cells with 200 μg/mL of the AHC-derived anthocyanin fraction increased p-AKT (Ser473) expression by approximately 2.70-fold, consistent with previous study findings. These findings suggest that the anthocyanin-rich fraction obtained from the purple wheat cultivar bran has significant antidiabetic activity, with glucose uptake rates and p-AKT (Ser473) expression similar to those observed in previous studies. Furthermore, the anthocyanin content of the purified anthocyanin-rich fraction was approximately eight times higher than the total anthocyanin content measured by RDA, and the C3OG content was approximately 230 times higher [16]. These results confirm successful purification, which is likely a key contributor to the observed antidiabetic activity of the anthocyanins.

AKT is a key regulator of glucose metabolism and is involved in various processes, including glucose transport, glycogen synthesis, and inhibition of gluconeogenesis [38]. The phosphorylation of AKT at Ser473, which occurs upon PI3K activation, is a key indicator of AKT pathway activity [39]. Previous studies have demonstrated that Ser473 phosphorylation serves as an indicator of the antidiabetic activity of the AKT pathway [7, 33, 40]. Future studies should further validate the antidiabetic activity by confirming the expression of downstream proteins in the AKT pathway.

In summary, this study successfully obtained anthocyanin-rich fractions from three purple wheat cultivars and evaluated their antioxidant and antidiabetic activities. A strong correlation was found between these activities and anthocyanin content. Notably, glucose uptake and AKT phosphorylation were the most prominent in the AHC fraction, followed by those in AJH and AH, reflecting the levels of major anthocyanins. These findings highlight a significant correlation between the metabolites of the anthocyanin-rich fraction of purple wheat and its antidiabetic activity. Overall, this study suggests that purple wheat serves as a promising functional food for the regulation of blood sugar levels in humans.

Methods

Chemicals and reagents

Amberlites XAD-7HP, 3-(4,5-dimethyl-2-thiazolyl)-2,5-diphenyltetrazolium bromide (MTT), and alpha-glucosidase were purchased from Sigma-Aldrich (St. Louis, MO, USA). High-glucose Dulbecco's modified Eagle medium (DMEM) and Dulbecco's phosphate-buffered saline (DPBS) were obtained from Biowest (France). Fetal bovine serum (FBS), penicillin-streptomycin (P/S), and N-2-hydroxyethylpiperazine-N'-2-ethanesulfonic acid (HEPES) were purchased from Gibco (Grand Island, NY, USA). Formic acid, MS-grade water, and acetonitrile were obtained from Thermo Fisher Scientific (Whatman,

MA, USA), and LC-grade methanol was obtained from Honeywell (Burdick & Jackson, USA). Cyanidin-3-O-glucoside was purchased from Chemfaces (Wuhan, Hubei, PRC) and peonidin-3-O-glucoside was purchased from Extrasynthese (Genay, Rhône, France). Cyanidin and cyanidin-3-rutinoside were purchased from Tokiwa (Tokyo, Japan).

Sample Preparation

Purple-wheat cultivars "Ariheuk", "Ari-jinheuk", and "Ariheukchal" were provided by the RDA of Korea in 2022 and stored at 4 ℃ until processing. Anthocyanins were isolated and purified as previously describe [17], with some modifications. The wheat grains were ground using a Roll mill (DK104, Korea) and sifted through a 40-mesh (425 μm) sieve. Each sample was mixed with n-hexane (1:15, v/v) and stirred for 2 h. The defatted samples were dried overnight under a fume hood and stored at -50 ℃. Samples (20 g) were extracted with acidified methanol (0.1% HCl in 80% methanol) at a 1:8 (w/v) ratio using bath sonication (3150 R-DTH sonicator, Branson, MO, USA) for 30 min, three times. Extracts were centrifuged at 20,001 × g for 10 min, filtered through Whatman No.1 filter paper (GE Healthcare, UK), and stored at -20 °C for 24 h to precipitate heavier molecules. The extracts were subjected to repeated centrifugation and filtration. They were then concentrated using rotary vacuum evaporation at 36 °C (Eyela, Tokyo, Japan).

Purification of anthocyanin-rich fraction

Fifty grams of ion-exchange resin (Amberlites XAD-7HP; particle size 20–60 mesh) was loaded into a glass column tube (2.2 cm x 30 cm) and swollen with methanol. The vacuum-concentrated acid-methanol phase was loaded onto the column. Next, the column was rinsed with 1 L of distilled water to remove sugars and organic acids. The anthocyanin components adsorbed onto the resin were eluted with 300 mL of acidified methanol (0.1% HCl in 80% methanol). The eluted anthocyanin fraction was concentrated using a rotary vacuum evaporator at 36 ℃, followed by speed-vac drying to yield an anthocyanin-rich fraction. The extracts were stored at -50 ℃ until use.

LC-MS/MS analysis

Compound analysis of the purple wheat cultivar-derived anthocyanin-rich fractions was performed using an UHPLC-HESI-Orbitrap MS/MS system. Specifically, compound analysis was performed with a Vanquish UHPLC system coupled to a Q Exactive™ Orbitrap MS/MS system (Thermo Scientific, Waltham, MA, USA), using a Thermo Hypersil Gold AQ C18 column (1.9 μm internal 100 × 2.1 mm) at 36 ℃ for chromatographic separation. The following gradient elution program was employed using 0.1% formic acid in water (A) and 0.1% formic acid in acetonitrile (B): 0–2 min, 5% B; 2–20 min, 5–40% B; 20–21 min, 40–90% B; 21–21.5 min, 90% B; 21.5–22 min, 90–5% B; 22–25 min, 5% B. The sample (5 μL) was injected into the system at a flow rate of 0.3 mL/min. Full MS scans were performed for each target component in positive ionization mode, with a scan range of 100–1200 m/z at a spray voltage of 3.80 kV.

Data processing and statistical analysis

LC-MS/MS data for anthocyanin profiling of the fractions obtained from purple-wehat cultivars were processed using Compound Discoverer 3.1 (Thermo Fisher Scientific, USA) with the following parameters: retention time of 0–25 min, alignment mass tolerance of 5 ppm, and a minimum peak intensity of 1×10^7. All raw data were filtered based on spectral properties using a signal-to-noise ratio threshold of > 3, followed by feature grouping parameters set to a retention time tolerance of ≤ 0.2 min. To support accurate compound annotation, the identities of target anthocyanin peaks were verified prior to quantification using external databases such as mzCloud (https://www.mzcloud.org/), MoNA (https://mona.fiehnlab.ucdavis.edu/), MASSBANK (www.massbank.jp), and PubChem (https://pubchem.ncbi.nlm.nih.gov) in combination with relevant literature. Data an alysis included heat map visualization and multivariate statistical analysis using SIMCA 17.0 (Umetrics, Umeå, Sweden).

The mean ± standard deviation (SD) of nine independent replicates is presented. Statistical analyses were performed using SPSS (version 12.0; IBM SPSS Statistics, Chicago, IL, USA), applying Duncan's test with $p < 0.05$ in one-way ANOVA. Anthocyanin profiling was conducted using SIMCA 17.0, with data analysis including principal component analysis (PCA) and hierarchical cluster analysis (HCA) to identify differences and similarities among the samples.

To evaluate the relationship between anthocyanin content and the observed biological activities, a Spearman's rank correlation analysis was performed using the quantified peak areas of four major anthocyanins and the corresponding values from antioxidant and antidiabetic assays. Spearman's correlation, a non-parametric statistical method, is suitable for identifying monotonic relationships between variables without assuming normal distribution. This method was chosen to account for potential non-linear associations and to ensure analytical robustness in interpreting biological relevance.

Phytochemical content measurement

The total phenolic content (TPC) in the purple-wheat-derived anthocyanin-rich fractions was assessed using a modified Folin & Ciocalteu method [41]. A reaction mixture was prepared by dissolving the sample in 0.2 M Folin

& Ciocalteu's reagent and 10% Na2CO3. The mixture was incubated at 37 ℃ for 1 h and absorbance was measured at 750 nm using a nanophotometer (IMPLEN, München, Germany). The TPC was calculated using gallic acid as a reference standard and expressed as mg of gallic acid equivalent (GAE) per g dry weight for each extract.

The total flavonoid content (TFC) of the anthocyanin-rich fractions was determined using an aluminum chloride ($AlCl_3$) colorimetric method, with quercetin as the reference standard [42]. A solution containing the diluted sample and distilled water was prepared, mixed with 5% $NaNO_2$, and allowed to stabilize for 5 min. Next, 10% $AlCl_3$ was added, and the mixture was incubated for 6 min. Finally, 1 M NaOH and distilled water were added. The absorbance was measured at 415 nm using a nanophotometer (IMPLEN, München, Germany). The TFC was expressed as mg quercetin equivalent (QE) per g dry weight for each extract.

TAC was assessed using the pH differential method [22]. The samples were diluted with 25 mM potassium chloride buffer (pH 1.0) and 0.4 M sodium acetate buffer (pH 4.5). The mixtures were allowed to equilibrate for 30 min before measuring the absorbance at 520 and 700 nm.

Cell culture

HepG2 (HB-8065) cells, a human liver cancer cell line, were cultured in high glucose DMEM (containing 10% FBS, 1% penicillin-streptomycin, and 1% HEPES) and incubated at 37 °C and 5% CO_2. The cells were maintained at approximately 70–80% confluence and passaged by washing with DPBS followed by detachment with trypsin. Subcultures were seeded at a density of 8.0×10^5 cells in 6 cm cell culture dishes.

In vitro model for IR

The IR cell model was established as previously described [33, 43], with some modifications. When HepG2 cells reached 70–80% confluence, the medium was replaced with serum free DMEM containing 4.5 g/L glucose and 1 μM insulin and the cells were further incubated for 24 h to induce IR. Subsequently, IR-HepG2 cells were treated with anthocyanin fractions at different concentrations (100, 200, 400 μg/mL) for 24 h, followed by treatment with 100 nM insulin for 20 min. Subsequently, a series of measurements were conducted.

Evaluation of cytotoxicity

Cytotoxicity was assessed using the MTT assay. HepG2 cells were seeded at a density of 1.0×10^4 cells/well in 96-well plates and incubated for 24 h. Samples were prepared by diluting the DMSO-dissolved extracts in DMEM, followed by incubation for 20 h. Treatment concentrations were 100, 200, and 400 μg/mL per extract. MTT reagent (1 mg/mL in DPBS, 20 μL) was added to each well and the cells were incubated for 4 h. Next, the medium was removed from all wells, and the formazan crystals were dissolved in 200 μL DMSO. Absorbance was measured at 570 nm using a microplate reader, and cytotoxicity was calculated relative to the viability of the control.

Evaluation of antioxidant activity

To evaluate the ability of the sample to scavenge pre-formed radicals, an in vitro DPPH assay was conducted [44]. Ascorbic acid (0.01–0.04 mM) served as a positive control. A 0.2 mM DPPH stock solution in methanol was prepared and stored in the dark. In a 96-well plate, the sample or ascorbic acid was mixed with the DPPH stock solution. The plate was incubated in the dark at 37 °C for 30 min, and absorbance was measured at 517 nm every 5 min using a microplate reader (SpectraMax M2, Molecular Devices, USA).

ABTS radical scavenging activity was assessed using a colorimetric method [45]. The ABTS cation radical was formed by reacting 2.4 mM potassium persulfate with 7 mM ABTS solution and incubation in the dark for 16 h. The working solution was diluted with distilled water to an absorbance of 0.7 ± 0.02 at 734 nm. The sample fraction and ABTS reagent were mixed and incubated in the dark for 30 min, and absorbance was measured at 734 nm using a microplate reader.

The Oxygen Radical Absorbance Capacity (ORAC) assay was performed using a modified method [46]. All chemicals and samples were dissolved in 75 mM phosphate buffer (pH 7.0). In a black 96-well plate, 3 μM fluorescein sodium salt and the sample were pre-incubated in the dark for 15 min at 37 °C. AAPH (221 mM) was then added, and fluorescence was recorded for 90 min at 1-min intervals (excitation at 485 nm and emission at 535 nm). Trolox (10–50 μM) was used as the standard antioxidant. ORAC was calculated based on the area under the curve (AUC) at 90 min.

Intracellular ROS levels

Intracellular ROS production was detected using the cell-permeant fluorogenic probe CM-H2DCFDA (Invitrogen, Carlsbad, CA, USA) as previously described [27], with some modifications. HepG2 cells were seeded in 96-well plates at 1×10^4 cells/well and incubated for 3 d. Following incubation, the cells were subjected to IR induction and sample treatment as described. After insulin treatment, cells were washed with DPBS, treated with 10 μM CM-H_2DCFDA, and incubated for 30 min. The cells were then rinsed three times with DPBS and resuspended in DPBS. Fluorescence was recorded at excitation and emission wavelengths of 492 and 522 nm, respectively. ROS

production was quantified and expressed as a percentage of control cells.

Evaluation of antidiabetic activity

α-Glucosidase inhibitory activity

The α-glucosidase inhibitory activity of anthocyanin-rich fractions was measured as previously described [47], with slight modifications. The sample, α-glucosidase enzyme solution (1.5 U/mL), and 50 mM potassium phosphate buffer (pH 6.8) were combined in a 96-well plate and pre-incubated at 37 °C for 5 min. After pre-incubation, 2.5 M pNPG (4-nitrophenyl α-D-glucopyranoside) was added, and absorbance was measured at 405 nm every minute for 20 min.

Glucose uptake assay

Glucose uptake was measured using the Glucose Uptake-Glo™ Assay kit (Promega, Madison, WI, USA), according to the manufacturer's instructions. IR was induced in HepG2 cells as previously described. After insulin treatment, 1 mM 2-DG (2-deoxyglucose) was added to each well, and the plate was incubated for 10 min at 25 °C The reaction was stopped by adding STOP buffer, followed by the addition of neutralization buffer and 2-DG6P detection reagent. After 1 h of incubation, luminescence was measured using a luminometer (GloMax® Discover Microplate Reader, Promega). Glucose uptake rates were compared between the low glucose-treated groups.

Western blotting for Akt expression for insulin signaling

Western blotting was performed to analyze the effect of the samples on insulin signaling via the PI3K/AKT pathway. HepG2 cells (8×10^5) were seeded in 6 cm dishes with high-glucose DMEM (25 mM). When the cells reached 70–80% confluence, IR was induced and samples were processed as described above cell culture method. The cells were rinsed with cold PBS, incubated on ice for 30 min, and lysed in RIPA buffer containing 1% protease and phosphatase inhibitors. The lysates were sonicated in ice-cold water for 30 s and then centrifuged at 16,000 × g for 15 min at 4 °C. The supernatants were collected. Protein (30 μg) from each sample were subjected to 8% SDS-PAGE, transferred onto a PVDF membrane (Invitrogen), and blocked with 5% BSA in TBST for 90 min. The membrane was incubated with primary antibodies (β-actin, Akt, p-Akt Ser473) at 4 °C for 24 h, washed with TBST, and exposed to secondary antibodies (anti-mouse IgG-HRP, anti-rabbit IgG-HRP) for 2 h at room temperature. Proteins were visualized using enhanced chemiluminescence (ECL) solution (Bio-Rad), detected with Amersham ImageQuant 800 (Cytiva), and quantified using ImageQuantTL (ver. 10.2; Cytiva).

Abbreviations

AH	Ariheuk
AJH	Ari-jinheuk
AHC	Ari-heukchal
BSA	Bovine serum albumin
C3OG	Cyanidin-3-O-glucoside
DMSO	Dimethyl sulfoxide
GAE	Gallic acid equivalent
HCl	Hydrochloric acid
HESI	Heated electrospray ionization
LC	Liquid chromatography
MS	Mass spectrometry
OPLS-DA	Orthogonal partial least squared-discriminant analysis
P3OG	Peonidin-3-O-glucoside
PCA	Principal component analysis
PC1	Principal component 1
PC2	Principal component 2
POS	Positive ionization
PRM	Parallel reaction monitoring
PVDF	Polyvinylidene fluoride
QE	Quercetin equivalen
RDA	Rural Development Administration
ROS	Reactive oxygen species
RT	Retention time
SD	standard deviation
SPSS	Statistical Package for the Social Science
TE	Trolox equivalent
TIC	Total ion chromatogram
UHPLC	Ultra high performance liquid chromatography

Acknowledgements
We thank the BT research facility center, Chung-Ang University.

Author contributions
YJC and JHA conceived and designed the experiments; YJC performed the experiments; YJC and JHA analyzed the data and wrote the manuscript.

Funding
This research was supported by a Chung-Ang University Graduate Research Scholarship (Academic scholarship for College of Biotechnology and Natural Resources).

Data availability
All data generated or analyzed during this study are included in this published article.

Declarations

Competing interests
The authors declare that they have no competing interests.

Received: 23 March 2025 / Accepted: 14 July 2025
Published online: 19 July 2025

References

1. Dangi P, Chaudhary N, Paul A, Sharma A, Dutta I, Razdan R, Pigmented, Wheat (2023) Nutrition scenario and health benefits. Pigmented cereals and millets: bioactive profile and food applications. The Royal Society of Chemistry, pp 1–26
2. Institute KWBIR (2020) Korean Wheat&Barley Industry Research Institute.;19
3. Jin H-Y, Jeon S-H, Kim K-H, Kang C-S, Choi H-S, Youn Y (2021) Phytochemical components and physiological activities of purple wheat Bran 'arriheuk'extracts. Food Sci Preservation 28(3):372–383
4. Garg M, Kaur S, Sharma A, Kumari A, Tiwari V, Sharma S et al (2022) Rising demand for healthy foods-anthocyanin biofortified colored wheat is a new research trend. Front Nutr 9:878221
5. Gupta R, Meghwal M, Prabhakar PK (2021) Bioactive compounds of pigmented wheat (Triticum aestivum): potential benefits in human health. Trends Food Sci Technol 110:240–252

6. Bowen-Forbes CS, Zhang Y, Nair MG (2010) Anthocyanin content, antioxidant, anti-inflammatory and anticancer properties of blackberry and raspberry fruits. J Food Compos Anal 23(6):554–560
7. Yan F, Dai G, Zheng X (2016) Mulberry anthocyanin extract ameliorates insulin resistance by regulating PI3K/AKT pathway in HepG2 cells and db/db mice. J Nutr Biochem 36:68–80
8. Su-Que L, Ya-Ning M, Xing-Pu L, Ye-Lun Z, Guang-Yao S, Hui-Juan M (2013) Effect of consumption of micronutrient enriched wheat steamed bread on postprandial plasma glucose in healthy and type 2 diabetic subjects. Nutr J 12:1–7
9. Reisinger M, Tirpanalan Ö, Huber F, Kneifel W, Novalin S (2014) Investigations on a wheat Bran biorefinery involving organosolv fractionation and enzymatic treatment. Bioresour Technol 170:53–61
10. Atwell WA, Finnie S (2016) Wheat flour. Elsevier
11. Olokoba AB, Obateru OA, Olokoba LB (2012) Type 2 diabetes mellitus: a review of current trends. Oman Med J 27(4):269
12. Miao L, Zhang H, Cheong MS, Zhong R, Garcia-Oliveira P, Prieto MA et al (2023) Anti-diabetic potential of apigenin, luteolin, and Baicalein via partially activating PI3K/Akt/Glut-4 signaling pathways in insulin-resistant HepG2 cells. Food Sci Hum Wellness 12(6):1991–2000
13. Dou Z, Liu C, Feng X, Xie Y, Yue H, Dong J et al (2022) Camel Whey protein (CWP) ameliorates liver injury in type 2 diabetes mellitus rats and insulin resistance (IR) in HepG2 cells via activation of the PI3K/Akt signaling pathway. Food Funct 13(1):255–269
14. He J-H, Chen L-X, Li H (2019) Progress in the discovery of naturally occurring anti-diabetic drugs and in the identification of their molecular targets. Fitoterapia 134:270–289
15. Hung H-Y, Qian K, Morris-Natschke SL, Hsu C-S, Lee K-H (2012) Recent discovery of plant-derived anti-diabetic natural products. Nat Prod Rep 29(5):580–606
16. Kim Kyung-hoon KK-m A new variety of wheat (KCTC18591P) and food composition for anti-oxidative activity comprising thereof. 10–2035666. Republic of Korea2019.
17. Abdel-Aal E-SM, Hucl P, Rabalski I (2018) Compositional and antioxidant properties of anthocyanin-rich products prepared from purple wheat. Food Chem 254:13–19
18. Forbes-Hernández TY, Gasparrini M, Afrin S, Cianciosi D, González-Paramás AM, Santos-Buelga C et al (2017) Strawberry (cv. Romina) methanolic extract and anthocyanin-enriched fraction improve lipid profile and antioxidant status in HepG2 cells. Int J Mol Sci 18(6):1149
19. Wang E, Yin Y, Xu C, Liu J (2014) Isolation of high-purity anthocyanin mixtures and monomers from blueberries using combined chromatographic techniques. J Chromatogr A 1327:39–48
20. Bourmaud A, Gallien S, Domon B (2016) Parallel reaction monitoring using quadrupole-Orbitrap mass spectrometer: principle and applications. Proteomics 16(15–16):2146–2159
21. Zhou J, Liu H, Liu Y, Liu J, Zhao X, Yin Y (2016) Development and evaluation of a parallel reaction monitoring strategy for large-scale targeted metabolomics quantification. Anal Chem 88(8):4478–4486
22. Hu C, Cai Y-Z, Li W, Corke H, Kitts DD (2007) Anthocyanin characterization and bioactivity assessment of a dark blue grained wheat (Triticum aestivum L. Cv. Hedong Wumai) extract. Food Chem 104(3):955–961
23. Knievel D, Abdel-Aal E-S, Rabalski I, Nakamura T, Hucl P (2009) Grain color development and the inheritance of high anthocyanin blue aleurone and purple pericarp in spring wheat (Triticum aestivum L). J Cereal Sci 50(1):113–120
24. Bustos DV, Riegel R, Calderini DF (2012) Anthocyanin content of grains in purple wheat is affected by grain position, assimilate availability and agronomic management. J Cereal Sci 55(3):257–264
25. Abdel-Aal ESM, Hucl P, Shipp J, Rabalski I (2016) Compositional differences in anthocyanins from blue-and purple-grained spring wheat grown in four environments in central Saskatchewan. Cereal Chem 93(1):32–38
26. Liu Q, Qiu Y, Beta T (2010) Comparison of antioxidant activities of different colored wheat grains and analysis of phenolic compounds. J Agric Food Chem 58(16):9235–9241
27. Yang Q, Zhu Z, Wang L, Xia H, Mao J, Wu J et al (2019) The protective effect of silk fibroin on high glucose induced insulin resistance in HepG2 cells. Environ Toxicol Pharmacol 69:66–71
28. Rains JL, Jain SK (2011) Oxidative stress, insulin signaling, and diabetes. Free Radic Biol Med 50(5):567–575
29. Wang Z, Sun L, Fang Z, Nisar T, Zou L, Li D et al (2021) Lycium ruthenicum Murray anthocyanins effectively inhibit α-glucosidase activity and alleviate insulin resistance. Food Bioscience 41:100949
30. Zhu W, Jia Q, Wang Y, Zhang Y, Xia M (2012) The anthocyanin cyanidin-3-O-β-glucoside, a flavonoid, increases hepatic glutathione synthesis and protects hepatocytes against reactive oxygen species during hyperglycemia: involvement of a cAMP–PKA-dependent signaling pathway. Free Radic Biol Med 52(2):314–327
31. Dai J, Ruan Y, Feng Y, Li B (2022) Physical properties, α-Glucosidase inhibitory activity, and digestive stability of four purple corn cob anthocyanin complexes. Foods 11(22):3665
32. Leclercq IA, Morais ADS, Schroyen B, Van Hul N, Geerts A (2007) Insulin resistance in hepatocytes and sinusoidal liver cells: mechanisms and consequences. J Hepatol 47(1):142–156
33. Wang M, Mao H, Chen J, Li Q, Ma W, Zhu N et al (2022) Chinese bayberry (Myrica rubra sieb. Et Zucc.) leaves proanthocyanidins alleviate insulin-resistance via activating PI3K/AKT pathway in HepG2 cells. J Funct Foods 99:105297
34. Huang X, Liu G, Guo J, Su Z (2018) The PI3K/AKT pathway in obesity and type 2 diabetes. Int J Biol Sci 14(11):1483
35. Chen Z, Li W, Guo Q, Xu L, Santhanam RK, Gao X et al (2019) Anthocyanins from dietary black soybean potentiate glucose uptake in L6 rat skeletal muscle cells via up-regulating phosphorylated Akt and GLUT4. J Funct Foods 52:663–669
36. Luna-Vital DA, Gonzalez de Mejia E (2018) Anthocyanins from purple corn activate free fatty acid-receptor 1 and glucokinase enhancing in vitro insulin secretion and hepatic glucose uptake. PLoS ONE 13(7):e0200449
37. Jiang X, Tang X, Zhang P, Liu G, Guo H (2014) Cyanidin-3-O-β-glucoside protects primary mouse hepatocytes against high glucose-induced apoptosis by modulating mitochondrial dysfunction and the PI3K/Akt pathway. Biochem Pharmacol 90(2):135–144
38. Whiteman EL, Cho H, Birnbaum MJ (2002) Role of akt/protein kinase B in metabolism. Trends Endocrinol Metabolism 13(10):444–451
39. Dai B, Wu Q, Zeng C, Zhang J, Cao L, Xiao Z et al (2016) The effect of Liuwei Dihuang Decoction on PI3K/Akt signaling pathway in liver of type 2 diabetes mellitus (T2DM) rats with insulin resistance. J Ethnopharmacol 192:382–389
40. Yan F, Zhang J, Zhang L, Zheng X (2016) Mulberry anthocyanin extract regulates glucose metabolism by promotion of glycogen synthesis and reduction of gluconeogenesis in human HepG2 cells. Food Funct 7(1):425–433
41. Singleton VL, Orthofer R, Lamuela-Raventós RM (1999) [14] Analysis of total phenols and other oxidation substrates and antioxidants by means of folin-ciocalteu reagent. Methods in Enzymology. Elsevier; pp. 152– 78
42. Alzand KI, Mohamed MA (2012) Flavonoids: chemistry, biochemistry and antioxidant activity. J Pharm Res 5(40134012):37
43. Huang Q, Chen L, Teng H, Song H, Wu X, Xu M (2015) Phenolic compounds ameliorate the glucose uptake in HepG2 cells' insulin resistance via activating AMPK: anti-diabetic effect of phenolic compounds in HepG2 cells. J Funct Foods 19:487–494
44. Marinova G, Batchvarov V (2011) Evaluation of the methods for determination of the free radical scavenging activity by DPPH. Bulgarian J Agricultural Sci 17(1):11–24
45. Re R, Pellegrini N, Proteggente A, Pannala A, Yang M, Rice-Evans C (1999) Antioxidant activity applying an improved ABTS radical cation decolorization assay. Free Radic Biol Med 26(9–10):1231–1237
46. Ou B, Hampsch-Woodill M, Prior RL (2001) Development and validation of an improved oxygen radical absorbance capacity assay using fluorescein as the fluorescent probe. J Agric Food Chem 49(10):4619–4626
47. Kim J-S, Hyun TK, Kim M-J (2011) The inhibitory effects of ethanol extracts from sorghum, Foxtail millet and proso millet on α-glucosidase and α-amylase activities. Food Chem 124(4):1647–1651

Publisher's note